Unified Mobility Model for Diffusion-Limited Current in Organic Diodes Based on Fermi-Dirac Statistics

Jiu-Xun Sun (孙久勋)⬤,* Hong-Chun Yang (杨宏春), Yang Li (李杨),† and Hai-Juan Cui (崔海娟)

School of Physics, University of Electronic Science and Technology of China, Chengdu 611731, China

The Fermi-Dirac statistics is adopted to consider degenerate effects in organic diodes. The degenerate drift-diffusion equation is analytically solved under the uniform-electrical-field approximation. The analytical expressions for the current-voltage relationship and carrier density are derived. The mobility model of Pasveer [Pasveer *et al.*, Phys. Rev. Lett. 94, 206601 (2005)] is improved to consider correct characteristic length scales and combined with the analytical solution to analyze the properties of six organic diodes. The theoretical results are in good agreement with experimental data. Six model parameters are extracted for six devices, namely, the parameters N_0 and σ for the density of states; the parameters μ_0 and a for the mobility model; and the potential barriers W_{an} and W_{cat} at the anode and cathode, respectively. The degenerate parameter $\bar{\eta}$ at 300 K is deduced. It is shown that two materials, MEH-PPV and F8BT, are degenerate. Although four other materials can be treated as nondegenerate, the degenerate effects are not negligible near the anode region.

I. INTRODUCTION

Organic semiconductors have attracted increasing attention in the last decade for wide electronic applications, such as displays, photovoltaics, lighting, or transistors. This is mainly due to the lower production cost, sustainability, and flexibility. It has been recognized that the optoelectronic properties of organic semiconductors are different from those of classical inorganic crystalline semiconductors. The most important problem here is an understanding of charge-transport processes in the materials. Charge transport in organic semiconductors is regarded as a hopping process between localized sites, which are thought to consist of conjugated polymer-chain segments. Variations in the on-site energies due to disorder are usually assumed to be Gaussian [1]. The most important transport parameter of an organic semiconductor is mobility. Theoretically, the mobility of organic semiconductors has been treated as a function of temperature T, electric field F, and charge density p [2]. The experimental mobility usually was extracted by the current-voltage (J-V) relationship for field-effect transistors [1] or organic diodes [2].

A popular structure of organic diodes is the metal-insulator-metal (*M-I-M*) structure. It is manufactured by sandwiching a layer of organic semiconductor between two electrodes. Previously, the J-V relationship of organic diodes was described by a space-charge-limited current (SCLC) equation proposed by Mott and Gurney [3]:

$$J = \frac{9}{8}\varepsilon\mu L^{-3}(V - V_{BI})^2 \tag{1}$$

with ε as the dielectric constant; μ as the charge-carrier mobility; L as the thickness of the organic layer; V as the applied voltage; and V_{BI} as the built-in voltage, $qV_{BI} = W_{cat} - W_{an}$, where W_{an} and W_{cat} are potential barriers at the anode and cathode, respectively. However, de Bruyn *et al.* [4] pointed out that the diffusion current was important not only at voltages below V_{BI} but also at those above V_{BI}. The Mott-Gurney equation ignores the diffusion current and is merely applicable to the condition with voltages far higher than V_{BI}. They [4] derived an analytical formula for diffusion-limited current in p-type organic *M-I-M* diodes:

$$J = \frac{q\mu N_v(V_{BI} - V)[\exp(qV/kT) - 1]}{L[\exp(qV_{BI}/kT) - \exp(qV/kT)]}, \tag{2}$$

where N_v is the effective density of states (DOS) for holes.

Equation (2) has been widely used to analyze the properties of organic diodes, including extraction of mobility μ [4–7], built-in voltage V_{BI} [8–10], etc. However, we notice that four physical factors are ignored in the derivation of Eq. (2). The first factor, the degeneracy effect, is ignored, and the Boltzmann statistics is used in the drift-diffusion equation. Although some reports in the literature supported the applicability of Boltzmann statistics to organic semiconductors [11,12], more and more works showed that

*sjx@uestc.edu.cn
†652106326@qq.com

the degeneracy effect was important, and the Fermi-Dirac statistics should be used in place of the Boltzmann statistics [13–16]. The second factor, the mobility μ, is treated as a constant independent of electric field F and density p, but the mobility of organic semiconductors is recognized as a function of $\mu(F,p)$ [1,2]. The third factor, the popular $\mu(F,p)$, of Pasveer et al. [2] is not universal, as pointed out by Nenashev et al. [17]. Parameters in $\mu(F,p)$ are treated as independent of the DOS and carrier density, but, in fact, parameters in these quantities are relevant for each other. The fourth factor is that Eq. (2) is derived by direct integration of the drift-diffusion equation, so the analytical expression of hole density, $p(x)$, is unavailable; this deficiency is inconvenient for some applications.

By taking the above four physical factors into account, we derive analytical solutions for the *M-I-M* organic diodes and improve the mobility model of Pasveer et al. [2]. Our model and solutions adopt the Fermi statistics, the function of $\mu(F,p)$, and can give an analytical expression of $p(x)$. We also modify the length scale of $\mu(F,p)$ [2] in terms of Ref. [17], and exhibit the relationship between the parameters in $\mu(F,p)$ with the DOS, $p(x)$, and drift-diffusion equation. This may impose strong constraints on the parameters, and the model is more physically reasonable. In Sec. II, we derive the analytical solutions. In Sec. III, we detail improvements of the mobility model. In Sec. IV, the model is applied to six devices. The conclusions are given in Sec. V.

II. DERIVATION OF SEMIANALYTICAL SOLUTION FOR *M-I-M* DIODES

The drift-diffusion equation under the Fermi statistics is as follows [4,13,14]:

$$J = qpF\mu(F,p) - kT\eta(p)\mu(F,p)\frac{dp}{dx}, \quad (3)$$

where $\eta(p)$ is the degeneracy coefficient due to the Fermi-Dirac statistics; it is a function of p. The boundary conditions of $p(x)$ under the Boltzmann statistics are as follows [4]:

$$p(0) = N_v\exp(-W_{an}/kT), \ p(L) = N_v\exp(-W_{cat}/kT). \quad (4)$$

Under the Fermi-Dirac statistics, the boundary conditions of $p(x)$ should be replaced by

$$p(0) = \int_{-\infty}^{\infty} \frac{G(E)dE}{1 + \exp[(W_{an} - E)/kT]}, \quad (5a)$$

$$p(L) = \int_{-\infty}^{\infty} \frac{G(E)dE}{1 + \exp[(W_{cat} - E)/kT]}. \quad (5b)$$

$G(E)$ is the Gaussian DOS with two parameters N_0 and σ:

$$G(E) = \left(N_0/\sigma\sqrt{2\pi}\right)\exp(-E^2/2\sigma^2). \quad (6)$$

If we expand Eq. (5) under nondegenerate conditions, we can obtain an expression for the effective DOS, $N_v = N_0\exp[\sigma^2/2(kT)^2]$. However, N_v is usually treated as a parameter independent of $G(E)$ [4–7]. This treatment is obviously unreasonable.

If the functions $\eta(p)$ and $\mu(F,p)$ are retained, Eq. (3) cannot be analytically solved. de Bruyn et al. [4] pointed out that there was no band bending in the *M-I-M* structure for the absence of space charge, and electric field F could be taken as a constant:

$$F = (V - V_{BI})/L. \quad (7)$$

Strictly speaking, the electric field should be determined by the Passion equation and is a function of position $F(x)$. de Bruyn et al. [4] have shown that the uniform-electric-field approximation, Eq. (7), is extremely good for typical *M-I-M* diodes, as the voltage is not larger than 10 V. Resulting Eq. (2) is in good agreement with numerical solutions adopting the Passion equation. We further replace $\eta(p)$ and $\mu(F,p)$ by the effective degeneracy coefficient, $\bar{\eta}$, and the average mobility, $\bar{\mu}$; their values should be determined consistently. Eq. (3) is changed to the following form:

$$J = qpF\bar{\mu} - kT\bar{\eta}\bar{\mu}\frac{dp}{dx}. \quad (8)$$

The integration of Eq. (8) gives

$$p(x) = \frac{J}{qF\bar{\mu}} + C\exp\left(\frac{qFx}{kT\bar{\eta}}\right). \quad (9)$$

Adopting the boundary condition of Eq. (5a), the integrating constant C can be determined:

$$p(x) = \frac{J}{qF\bar{\mu}} + \left[p(0) - \frac{J}{qF\bar{\mu}}\right]\exp\left(\frac{qFx}{kT\bar{\eta}}\right). \quad (10)$$

Applying the boundary condition of Eq. (5b) to Eq. (10), we can solve the current as

$$J = \frac{qF\bar{\mu}\{p(0) - p(L)\exp[-(qFL/kT\bar{\eta})]\}}{1 - \exp[-(qFL/kT\bar{\eta})]}. \quad (11)$$

Substitution of Eq. (11) into Eq. (10) yields

$$p(x) = p(L) + [p(0) - p(L)]\frac{1 - \exp[qF(x - L)]/kT\bar{\eta}}{1 - \exp[-(qFL/kT\bar{\eta})]}. \quad (12)$$

Equations (11) and (12) are applicable to the case with $F > 0$. For the case with $F < 0$, Eqs. (11) and (12) should
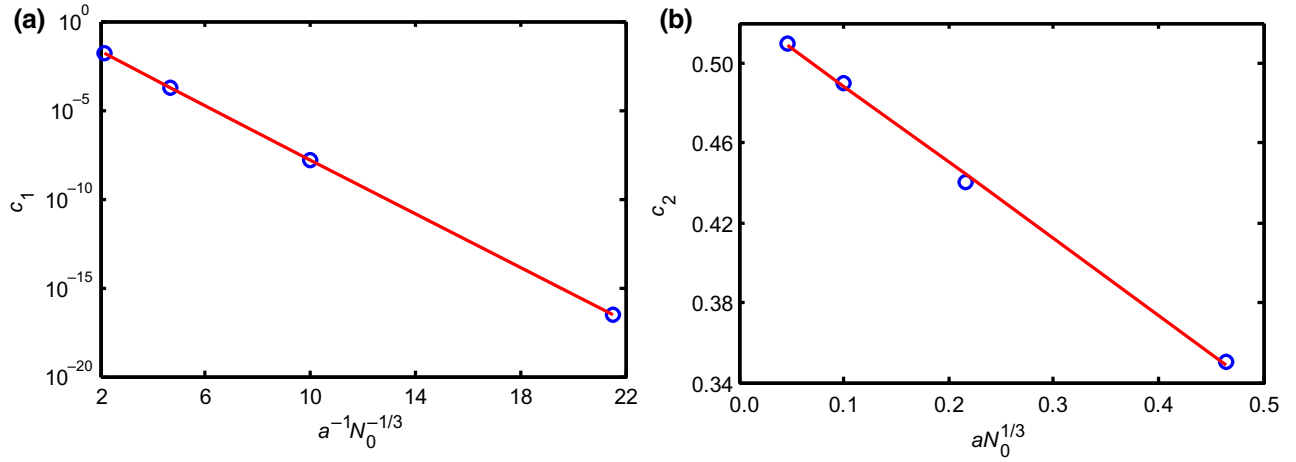
FIG. 1. Comparison of fitting curves from Eq. (22) (solid lines) with simulated data [19] (symbols) for two coefficients, c_1 and c_2, versus $aN_0^{1/3}$.

be mathematically changed to avoid the possibility of divergence in numerical calculations.

To determine the value of $\bar{\eta}$, we adopt the condition, $J = 0$, as $V = 0$. As applying the condition to Eq. (11), we have

$$J \propto p(L) - p(0)\exp\left(-\frac{qV_{BI}}{kT\bar{\eta}}\right) = 0.$$

The value of $\bar{\eta}$ is solved as

$$\bar{\eta} = \frac{qV_{BI}}{kT\ln[p(0)/p(L)]}. \tag{13}$$

Equation (13) shows that the effective degeneracy coefficient, $\bar{\eta}$, is determined by the carrier densities $p(0)$ and $p(L)$ at the anode and cathode. If $p(0)$ and $p(L)$ are taken in Eq. (4) under Boltzmann statistics, then $\bar{\eta}$ should have a value of one under nondegenerate conditions. The value of $\bar{\mu}$ should be evaluated as the following average:

$$\bar{\mu} = L^{-1} \int_0^L \mu[F, p(x)]\,dx. \tag{14}$$

III. IMPROVEMENT OF UNIFIED MOBILITY MODEL

The mobility function, $\mu(F,p)$, used in this work is the expression proposed by Pasveer et al. [2] through fitting the numerical solution of the master equation

$$\mu(T,p,F) = \mu(T,p)f(T,F), \tag{15}$$

$$\mu(T,p) = \mu_0 c_1 \exp(-c_2\hat{\sigma}^2)\exp\left[\frac{1}{2}(\hat{\sigma}^2 - \hat{\sigma})(2pb^3)^\delta\right], \tag{16}$$

$$c_1 = 1.8 \times 10^{-9}, c_2 = 0.42,$$

$$\delta = 2\hat{\sigma}^{-2}[\ln(\hat{\sigma}^2 - \hat{\sigma}) - \ln(\ln 4)], \tag{17}$$

$$f(T,F) = \exp\left\{0.44(\hat{\sigma}^{3/2} - 2.2)\left[\sqrt{1 + 0.8(qFb/\sigma)^2} - 1\right]\right\}, \tag{18}$$

with $\hat{\sigma} = \sigma/kT$, $\mu_0 = qv_0b^2/\sigma$, and b is the lattice constant. In solving the master equation, Pasveer et al. [2]

TABLE I. Thickness, L, of active layer; optimized parameters N_0, σ, μ_0, a, W_{an}, and W_{cat}; and deduced parameter $\bar{\eta}$ at 300 K for six organic diodes.

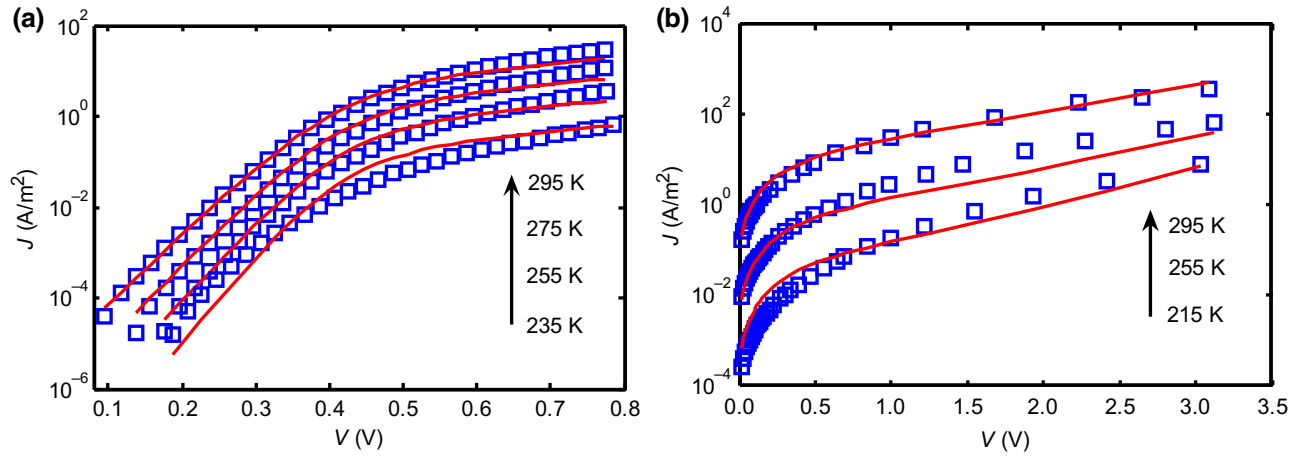|	PFO [4]	MEH-PPV [5]	F8BT [20]	2-TNATA [21]	Spiro-TAD [21]	TCTA [21]
L (nm)	80	100	74	151	179	179
N_0 (m^{-3})	1.103×10^{26}	1.445×10^{26}	5.018×10^{26}	3.362×10^{26}	1.721×10^{26}	1.721×10^{26}
σ (eV)	0.05	0.293	0.23	0.08	0.06	0.08
μ_0 (m^2/Vs)	1.105×10^{-4}	1.455×10^{8}	89.76	2.233×10^{-4}	5.234×10^{-4}	8.723×10^{-5}
a (nm)	0.58	0.53	0.35	0.4	0.5	0.5
W_{an} (eV)	0.35	1.35	0.9	0.37	0.32	0.31
W_{cat} (eV)	0.76	1.4	1.0	0.5	0.5	0.6
$\bar{\eta}$	1.00	3.28	2.13	1.02	1.00	1.03

FIG. 2. Comparison of theoretical curves (solid lines) with experimental data (symbols) for devices made from the materials PFO [4] (a) and MEH-PPV [5] (b).

have assumed a cubic lattice and taken $b = 10a$. Here, a is the localization length of charges in the Miller-Abrahams hopping rates, and ν_0 is the trying frequency,

$$W_{ij} = \begin{cases} \nu_0 \exp[-2r_{ij}/a - \beta(\varepsilon_i - \varepsilon_j)], & \varepsilon_j \geq \varepsilon_i, \\ \nu_0 \exp[-2r_{ij}/a], & \varepsilon_j < \varepsilon_i. \end{cases} \quad (19)$$

The mobility model in Eqs. (15)–(18) has three independent parameters: μ_0, σ, and b.

Nenashev *et al.* [17] pointed out that the fundamental characteristic length scale for the field dependence of mobility in disordered organic semiconductors should be the localization length, a, of charges rather than the lattice constant, b. So, the mobility model in Eqs. (15)–(18) should be modified in accordance with the conclusion of Nenashev *et al.* [17]. Upreti *et al.* [18] made extensive kinetic Monte Carlo calculations and surprisingly found that the mobility model of Pasveer *et al.* [2] was in good agreement with the Monte Carlo calculations and

extremely successful, despite it being based on the assumption of nearest-neighbor hopping on a regular lattice. Lee *et al.* [19] recently made detailed simulations under wider parameter ranges and found that the mobility model of Pasveer *et al.* [2] was qualitatively in agreement with their simulation data; quantitative agreement can be accessible if the parameters are slightly adjusted.

We think three modifications should be made in accordance with Refs. [17,19]. Pasveer *et al.* [2] have assumed a cubic lattice; the lattice number density, N_0, can be expressed as $N_0 = b^{-3}$. Lee *et al.* [19] proposed and verified the first modification: parameter b in Eq. (16) should be replaced by N_0. Then Eq. (16) is changed to following form:

$$\mu(T, p) = \mu_0 c_1 \exp(-c_2 \hat{\sigma}^2) \exp\left[\frac{1}{2}(\hat{\sigma}^2 - \hat{\sigma})(2p/N_0)^\delta\right], \quad (20)$$
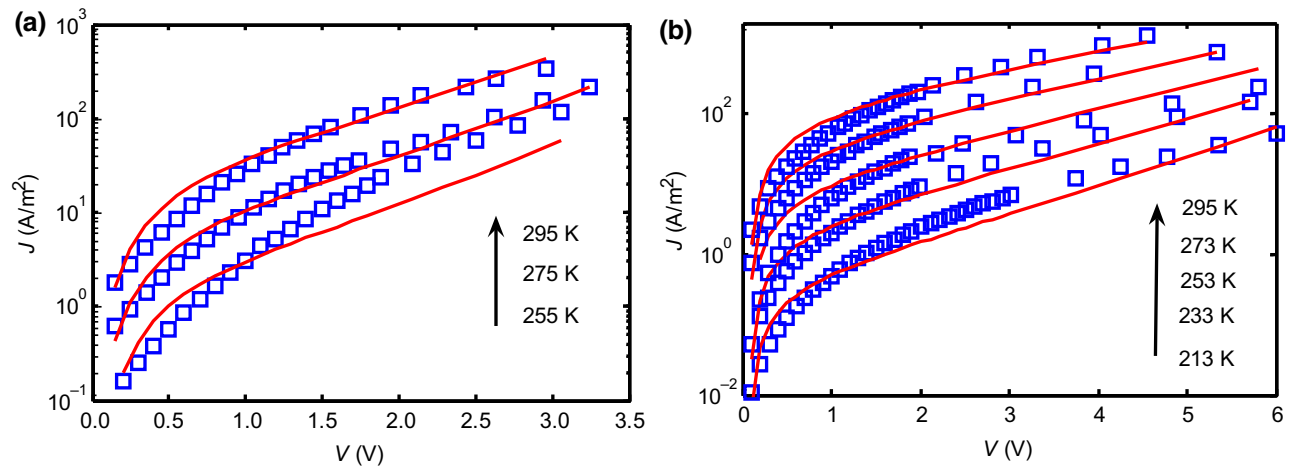

FIG. 3. Comparison of theoretical curves (solid lines) with experimental data (symbols) for devices made the materials F8BT [20] (a) and 2-TNATA [21] (b).
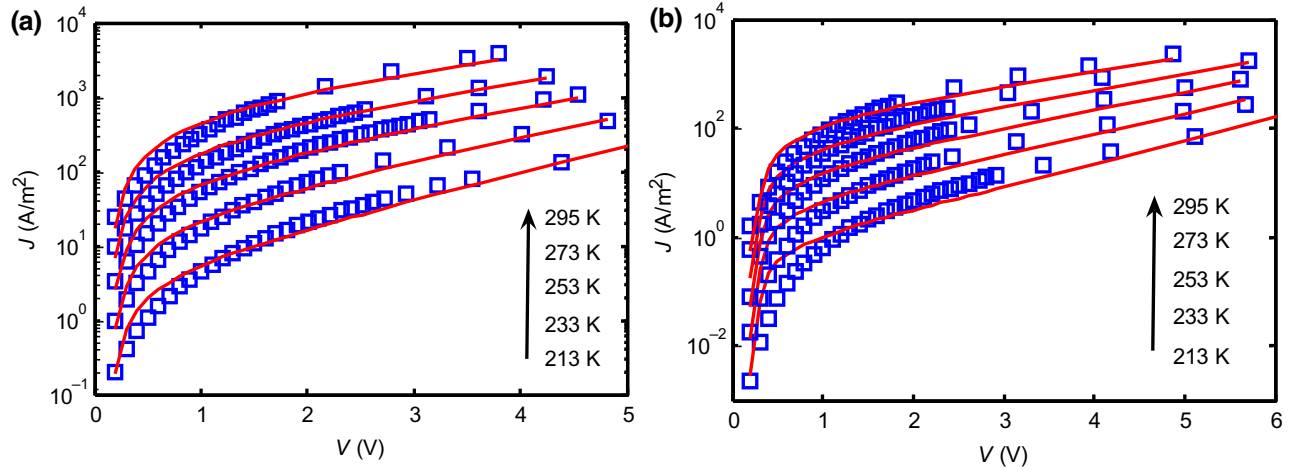
FIG. 4.　Comparison of theoretical curves (solid lines) with experimental data (symbols) for devices made from materials Spiro-TAD [21] (a) and TCTA [21] (b).

with $\mu_0 = qv_0 N_0^{-2/3}/\sigma$. We think that the modification in Eq. (20) is necessary, since N_0 is the total density of sites in the DOS of Eq. (6). Equation (20) evidently exhibits the relationship of N_0 with mobility; in contrast with original expressions of Pasveer *et al.* [2], where it is independent of N_0.

The second modification is that the lattice constant, b, should be replaced by the localization length, a. Since Pasveer *et al.* have taken $b = 10a$ in their simulations, we should substitute this relationship into Eq. (18) and treat a as an independent parameter:

$$f(T,F) = \exp\left\{0.44(\hat{\sigma}^{3/2} - 2.2)\left[\sqrt{1 + 80(qFa/\sigma)^2} - 1\right]\right\}.$$
$$(21)$$

Although the replacement of b by a in Eq. (21) is not strict, it is reasonable for three reasons. The first reason is that Nenashev *et al.* [17] pointed out that the fundamental characteristic length scale of the field dependence of mobility should be a rather than b. The second reason can also be deduced from simulation results of Nenashev *et al.* [17] that the changing amplitude of mobility versus b is more remarkable than that of a. This implies that the changing range of a is smaller than that of b for practical organic semiconductors. So, the replacement of b by a in Eq. (21) is acceptable. The third reason is that the simulations of Pasveer *et al.* [2] are based on the Miller-Abrahams hopping rates, Eq. (19). The localization length, a, is a fundamental parameter in the Miller-Abrahams hopping rates and must appear in the reasonable mobility expression. The original mobility expression in Eqs. (15)–(18) has nothing
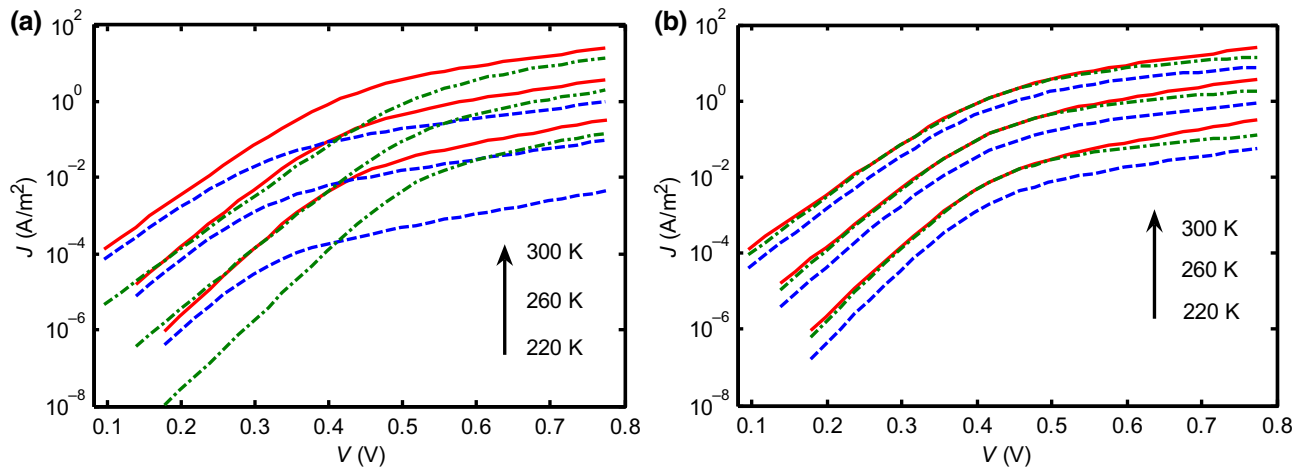

FIG. 5.　Theoretical curves at three temperatures, 220, 260, and 300 K, for devices made from PFO [4], with all parameters taking values given in Table I, except for other one parameter: (a) with $W_{an} = 0.5$ eV (dashed lines) and $W_{cat} = 0.9$ eV (dotted-dashed lines), and (b) with $\sigma = 0.05$ eV (dashed lines) and $a = 0.5$ nm (dotted-dashed lines).
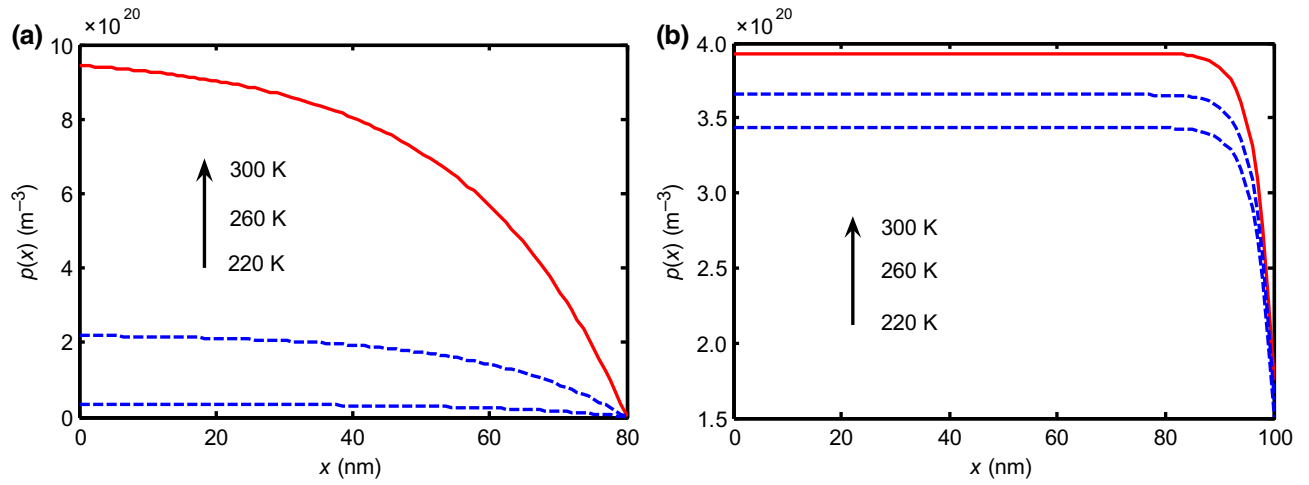
FIG. 6. Theoretical curves, $p(x)$, for devices made from PFO at 0.5 V [4] (a) and MEH-PPV at 2 V [10] (b), at 220, 260, and 300 K.

to do with a; this is unreasonable. Revised Eq. (21) can overcome such unreasonableness.

The third modification is as follows. Two coefficients, c_1 and c_2, in original Eq. (17) of Pasveer et al. [2] are taken as fixed constants. Lee et al. [19] extracted values of c_1 and c_2 based on their simulation data under wider parameter ranges and found that c_1 and c_2 should be dependent on N_0. Their simulations give values of $c_1 = 1.54 \times 10^{-2}$, 1.86×10^{-4}, 1.62×10^{-8}, and 2.75×10^{-17} and $c_2 = 0.35$, 0.44, 0.49, and 0.51, for values of $N_0 a^3 = 10^{-1}$, 10^{-2}, 10^{-3}, and 10^{-4}, respectively. Considering that the value of $N_0 a^3$ should be a continuous variable in practical situations, we carefully analyze these data and deduce the following simple expressions:

$$c_1 = \exp(-0.4338 - 1.7501 a^{-1} N_0^{-1/3}), \tag{22a}$$

$$c_2 = 0.5268 - 0.384 a N_0^{1/3}. \tag{22b}$$

Equation (22) is compared with simulation data in Fig. 1, which shows that the agreement is excellent.

The improved mobility model in Eqs. (15), (17), and (20)–(22) has four independent parameters: μ_0, σ, N_0, and a. Upon combining our M-I-M J-V formula with the original mobility model of Pasveer et al., we have six parameters: N_0, μ_0, σ, b, W_{an}, and W_{cat}. We also have six parameters with the improved mobility model of Pasveer et al.: N_0, μ_0, σ, a, W_{an}, and W_{cat}. We think that Eq. (22) should be considered in revised Eq. (20). Because current Eq. (11) is in proportion to the product, $\mu_0 N_0$, if Eq. (22) were not adopted in the revised mobility models, then we could merely determine the product $\mu_0 N_0$ but could not determine respective values of μ_0 and N_0. This implies that one redundant parameter exists among N_0 and μ_0, if ignoring Eq. (22). Whereas the six parameters become independent from each other, once considering Eq. (22), and can be determined by fitting experimental J-V data.
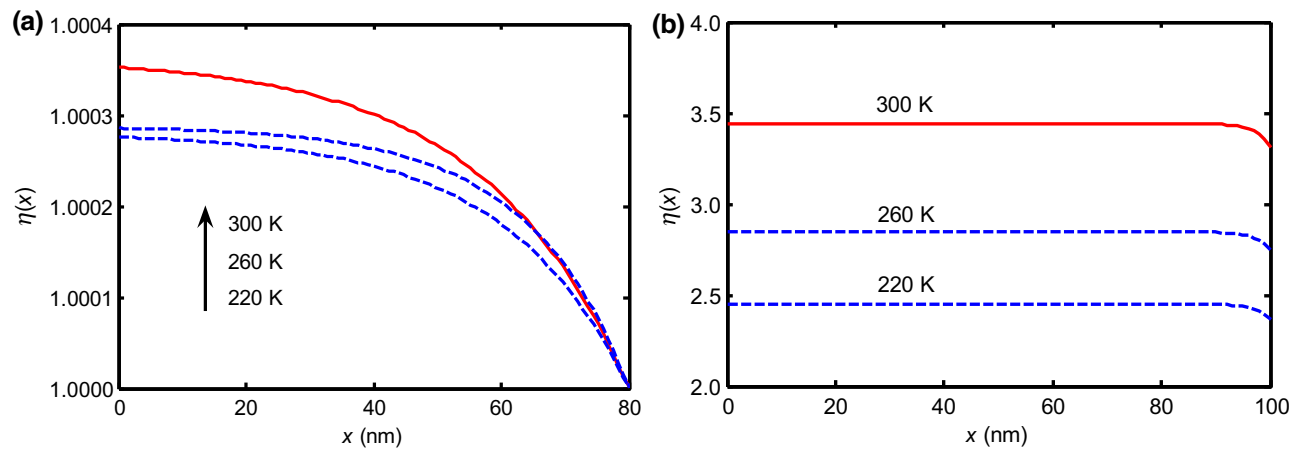

FIG. 7. Theoretical curves, $\eta(x)$, for devices made from PFO at 0.5 V [4] (a) and MEH-PPV at 2 V [5] (b) at 220, 260, and 300 K.

IV. NUMERICAL RESULTS AND DISCUSSION

In this section, we apply the above model and formula to six diodes fabricated by using different materials. Experimental data are taken from Ref. [4] for poly(9,9-dioctylfluorene) (PFO); 270 Ref. [5] for poly[2-methoxy-5-(2- ethylhexyloxy)-1,4-phenylenevinylene] (MEH-PPV); Ref. [20] for poly(9,9-dioctylfluorene-alt-BT) (F8BT); and Ref. [21] for 4,4',4''-tris[2-naphthyl(phenyl)amino] triphenylamine (2-TNATA), 2,2',7,7'-tetrakis(N,N-diphenylamino)-9,9-spirobifluorene (Spiro-TAD), and tris(4-carbazoyl-9-ylphenyl)amine (TCTA). The thickness of the organic layer and six model parameters are listed in Table I, which show that the values of extracted parameters are reasonable. The reason for a large varying range of μ_0 is due to prefactor c_1 of Eq. (22a) being fairly sensitive to $N_0 a^3$, as shown in Fig. 1(a). If including prefactor c_1 of Eq. (20) in μ_0, the varying range of $\mu_0 c_1$ would be reduced.

Comparisons of fitting curves with experimental data are shown in Figs. 2–4 for the six devices. Figures 2–4 show that the agreement of the results from our model with experimental data is satisfactory. The results for F8BT in Fig. 3(a) and TCTA in Fig. 4(b) are slightly unsatisfactory. This may be because of three reasons. The first reason is that the final transport mechanism or mobility model have not been found, although several popular mobility models have been proposed [17–19]. The second reason is that the theoretical J-V results at low voltage are very sensitive to potential barriers, but the barriers are dependent on temperature [22] or other factors [23]. The third reason is that the contacts are possibly not ohmic. For example, Lous *et al.* [24], Haldi *et al.* [25], and Yampolskii *et al.* [26] have shown that the electrodes of organic devices are possibly Schottky contacts; hot-carrier emission at contacts should be considered to describe J-V data of diodes. Tang *et al.* [27] proposed a strategy to form ohmic contacts for organic devices. Lopez-Varo *et al.* [28] proposed that the carrier density at contacts for the nonohmic contacts should be a power function of current, $p_{contact} = K_1 J_{contact}^m + K_2$, with three parameters: m, K_1, and K_2. It is our next working aim to combine the general boundary conditions into our model.

To analyze the influence of the parameters on the J-V curves, in Fig. 5, we plot variations of J-V curves versus the parameters W_{an}, W_{cat}, σ, and a. Figure 5(a) shows that the J-V curves decrease if all other parameters are kept unchanged, except for one parameter, W_{an}, which increases from 0.4 to 0.5 eV, and W_{cat} increases from 0.8 to 0.9 eV, respectively. It can be seen that the shape of the J-V curves at the high-voltage side is more sensitive to W_{an}, whereas the shape of the J-V curves at the low-voltage side is more sensitive to W_{cat}. Figure 5(b) shows that the J-V curves move down as σ decreases from 0.1 to 0.05 eV. The extent of movement at low temperature is more evident than that at high temperature. The J-V curves move down at the low-

and high-voltage sides as a decreases from 1.8 to 0.5 nm, and the extent of movement at the high-voltage side is more evident than that at the low-voltage side.

In the last line of Table I, we list the values of $\bar{\eta}$ at 300 K. Table I shows that the values of the parameter $\bar{\eta}$ for four devices, PFO, 2-TNATA, Spiro-TAD, and TCTA, are very close to one, so the degeneracy effect is possibly not important for these four devices. But the parameter $\bar{\eta}$ for the other two devices, MEH-PPV and F8BT, is far larger than one, so the two devices are degenerate. Table I also shows that the values of σ for two devices, MEH-PPV and F8BT, are far larger than those of the other four devices, so it can be postulated that the degeneracy is mainly related to the value of parameter σ. The larger the value of σ is, the stronger the degeneracy is.

In Figs. 6 and 7, we plot curves of carrier density, $p(x)$, and degeneracy, $\eta(x)$, for two devices, PFO and MEH-PPV, at three temperatures. Figure 6 shows that the $p(x)$ curves for the PFO device are more gradual than those of the MEH-PPV device. The $p(x)$ is a decreasing function of x, because W_{cat} is larger than W_{an}, and the threshold voltage, $qV_{BI} = W_{cat} - W_{an}$, is positive. Figure 7 shows that $\eta(x)$ is a decreasing function of x and temperature, but the difference between the values of the PFO and MEH-PPV devices is very large. The value, 1.00, of $\bar{\eta}$ at 300 K for the PFO device is very close to one; the value of $\eta(x)$ near the anode is slightly larger than one. The PFO device can be treated as nondegenerate. For the MEH-PPV device, the value of $\bar{\eta}$ at 300 K is 3.28; it should be degenerate. It is meaningful to explore other properties of the MEH-PPV material and devices, since it is evidently different from other materials.

V. CONCLUSIONS

The Fermi-Dirac statistics is adopted to consider the degenerate effects. The degenerate drift-diffusion equation is analytically solved under the uniform-electrical-field approximation. The analytical expressions for the current-voltage relationship and carrier density are derived. The mobility model of Pasveer *et al.* is improved to consider correct characteristic length scales and combined with the analytical solution to analyze the properties of six organic diodes. The theoretical results are in good agreement with experimental data. Six materials and device parameters are extracted, namely, N_0, σ, μ_0, a, W_{an}, and W_{cat}, and degenerate parameter $\bar{\eta}$ at 300 K is deduced. It is shown that two materials, MEH-PPV and F8BT, are degenerate. Although four other materials can be treated as nondegenerate, the degenerate effects are not negligible near the anode.

---

[1] M. C. J. M. Vissenberg and M. Matters, Theory of the field-effect mobility in amorphous organic transistors, Phys. Rev. B **57**, 12964 (1998).

[2] W. F. Pasveer, J. Cottaar, C. Tanase, *et al.*, Unified Description of Charge-Carrier Mobilities in Disordered Semiconducting Polymers, Phys. Rev. Lett. **94**, 206601 (2005).

[3] N. F. Mott and R. W. Gurney, *Electronic Processes in Ionic Crystals* (Dover, New York, 1964).

[4] P. de Bruyn, A. H. P. van Rest, G. A. H. Wetzelaer, D. M. de Leeuw, and P. W. M. Blom, Diffusion-Limited Current in Organic Metal-Insulator-Metal Diodes, Phys. Rev. Lett. **111**, 186801 (2013).

[5] G. A. H. Wetzelaer and P. W. M. Blom, Ohmic current in organic metal-insulator-metal diodes revisited, Phys. Rev. B **89**, 241201(R) (2014).

[6] A. K. Muhammad and J. X. Sun, Improved model for diffusion-limited current in organic metal-insulator-metal diodes, RSC Adv. **5**, 18720 (2015).

[7] J. A. Röhr, X. Y. Shi, S. A. Haque, T. Kirchartz, and J. Nelson, Charge Transport in Spiro-OMeTAD Investigated Through Space-Charge-Limited Current Measurements, Phys. Rev. Appl. **9**, 044017 (2018).

[8] S. Dahlström, O. J. Sandberg, M. Nyman, and R. Österbacka, Determination of Charge-Carrier Mobility and Built-in Potential in Thin-Film Organic M-I-M Diodes From Extraction-Current Transients, Phys. Rev. Appl. **10**, 054019 (2018).

[9] J. A. Röhr, Direct Determination of Built-in Voltages in Asymmetric Single-Carrier Devices, Phys. Rev. Appl. **11**, 054079 (2019).

[10] G. A. H. Wetzelaer, Improved Determination of the Mobility and Built-in Voltage in Asymmetric Single-Carrier Devices, Phys. Rev. Appl. **13**, 034069 (2020).

[11] G. A. H. Wetzelaer, L. J. A. Koster, and P. W. M. Blom, Validity of the Einstein Relation in Disordered Organic Semiconductors, Phys. Rev. Lett. **107**, 066605 (2011).

[12] C. X. Zhou, J. X. Sun, Z. J. Deng, and S. Zhou, Study of applicability of Boltzmann-statistics and two mobility models for organic semiconductors, Semiconductors **47**, 1351 (2013).

[13] Y. Roichman and N. Tessler, Generalized Einstein relation for disordered semiconductors -implications for device performance, Appl. Phys. Lett. **80**, 1948 (2002).

[14] L. Li, N. D. Lu, M. Liu, *et al.*, General Einstein relation model in disordered organic semiconductors under quasiequilibrium, Phys. Rev. B **90**, 214107 (2014).

[15] X. H. Shi, J. X. Sun, and Ch. H. Xiong, Dependence of general Einstein relation on density of state for organic semiconductors, Org. Electron. **35**, 65 (2016).

[16] A. Abutaha, P. Kumar, E. Yildirim, W. Shi, S. W. Yang, G. Wu, and K. Hippalgaonkar, Correlating charge and thermoelectric transport to paracrystallinity in conducting polymers, Nat. Commun. **11**, 1737 (2020).

[17] A. V. Nenashev, J. O. Oelerich, A. V. Dvurechenskii, F. Gebhard, and S. D. Baranovskii, Fundamental characteristic length scale for the field dependence of hopping charge transport in disordered organic semiconductors, Phys. Rev. B **96**, 035204 (2017).

[18] T. Upreti, Y. M. Wang, H. T. Zhang, D. Scheunemann, F. Gao, and M. Kemerink, Experimentally Validated Hopping-Transport Model for Energetically Disordered Organic Semiconductors, Phys. Rev. Appl. **12**, 064039 (2019).

[19] Y. J. Lee, S. Y. Jung, A. Plews, A. Nejim, O. Simonetti, L. Giraudet, S. D. Baranovskii, F. Gebhard, K. Meerholz, S. J. Jung, G. Horowitz, and Y. Bonnassieux, Parametrization of the Gaussian Disorder Model to Account for the High Carrier Mobility in Disordered Organic Transistors, Phys. Rev. Appl. **15**, 024021 (2021).

[20] Y. Zhang and P. W. M. Blom, Electron and hole transport in poly(fluorene-benzothiadiazole), Appl. Phys. Lett. **98**, 143504 (2011).

[21] N. B. Kotadiya, A. Mondal, Shiyun Xiong, P. W. M. Blom, D. Andrienko, and G.-J. A. H. Wetzelaer, Rigorous characterization and predictive modeling of hole transport in amorphous organic semiconductors, Adv. Electron. Mater. **4**, 1800366 (2018).

[22] M. Kemerink, J. M. Kramer, H. H. P. Gommans, and R. A. J. Janssen, Temperature-dependent built-in potential in organic semiconductor devices, Appl. Phys. Lett. **88**, 192108 (2006).

[23] F. Neumann, Y. A. Genenko, C. Melzer, S. V. Yampolskii, and H. von Seggern, Self-consistent analytical solution of a problem of charge-carrier injection at a conductor/insulator interface, Phys. Rev. B **75**, 205322 (2007).

[24] E. J. Lous, P. W. M. Blom, L. W. Molenkamp, and D. M. de Leeuw, Schottky contacts on a highly doped organic semiconductor, Phys. Rev. B **51**, 17251 (1995).

[25] A. Haldi, A. Sharma, W. J. Potscavage, Jr., and B. Kippelen, Equivalent circuit model for organic single-layer diodes, J. Appl. Phys. **104**, 064503 (2008).

[26] S. V. Yampolskii, Yu. A. Genenko, C. Melzer, K. Stegmaier, and H. von Seggern, Bipolar charge-carrier injection in semiconductor/insulator/conductor heterostructures: Self-consistent consideration, J. Appl. Phys. **104**, 073719 (2008).

[27] C. G. Tang, M. C. Y. Ang, K. K. Choo, V. Keerthi, J. K. Tan, M. Nur Syafiqah, T. Kugler, J. H. Burroughes, R. Q. Png, L. L. Chua, and P. K. H. Ho, Doped polymer semiconductors with ultrahigh and ultralow work functions for ohmic contacts, Nature **539**, 526 (2016).

[28] P. Lopez-Varo, J. A. Jiménez-Tejada, O. Marinov, C. H. Chen, and M. J. Deen, Charge density at the contacts of symmetric and asymmetric organic diodes, Org. Electron. **35**, 74 (2016).